Supplementary Data

General

Buffers including 0.1 M phosphate buffered saline (PBS), pH 7.5, 0.2 M ammonium acetate, pH 5.5, and 0.2M citric acid pH 2 were prepared from chemicals purchased from Merck (Darmstadt, Germany). High-quality Milli-Q water (resistance higher than 18 MΩ x cm) was used for preparing the solutions. Buffers, which were used for conjugation and labeling, were purified from metal contamination using Chelex 100 resin (Bio-Rad Laboratories, Hercules, CA, USA). ^{111}In-indium chloride (in 0.05 M HCl) was purchased from Mallinckrodt plc (Dublin, Ireland). ^{125}I was purchased from PerkinElmer (Waltham, USA).
In all iodination experiments, freshly prepared water solutions of Chloramine-T, N-chloro-p-toluenesulfonamide sodium salt, and sodium metabisulfite ($Na_2S_2O_5$) were used, both from Sigma (St. Louis, MO, USA).

Labeling yield and radiochemical purity of the labeled conjugates was determined by radio-ITLC using 150-771 DARK GREEN strips (Biodex Medical Systems, New York, NY, USA) eluted with 0.2 M citric acid for indium-labeled and acetone (80%) for iodinated conjugates. In this system, free radionuclide migrates with the solvent front and the radiolabeled conjugate stays at the application point. Sodium dodecyl sulfate polyacrylamide gel electrophoresis (SDS-PAGE) using NuPAGE 4–12% Bis-Tris Gel (Invitrogen AB, Lidingö, Sweden) in MES buffer (Invitrogen AB) was used for cross-validation of stability results. The distribution of radioactivity along the thin layer chromatography strips and SDS-PAGE gels was measured on a Cyclone Storage Phosphor System and analyzed using the OptiQuant software (Perkin Elmer Wellesey, MA, USA).

The radioactivity uptake in the cellular processing and the biodistribution studies was measured using an automated gamma-counter with 3 inch NaI(TI) detector (1480 WIZARD, Wallac, Turku).

The data were analyzed by an unpaired, two-tailed *t*-test using GraphPad Prism (version 4.00 for Windows GraphPad Software, San Diego, USA), in order to determine significant differences ($P<0.05$).

Radiolabelling and stability testing

For labeling of $Z_{HER2:342}$-SR-*HP1* and *HP2* with ^{111}In, the lyophilized conjugate (50 µg) was reconstituted in 20-140 µL 0.2 M ammonium acetate, pH 5.5, mixed with 3-30 MBq ^{111}In stock solution and incubated at 90^{o}C for 30 min. After labeling, the radio-conjugates were purified using a NAP-5 size-exclusion column equilibrated with PBS, if necessary.

Measurements of labeling yield and radiochemical purity of the conjugates were performed by radio-instant thin layer chromatography (ITLC) cross-validated by radio-SDS-PAGE (200 V constant) (Figures S1-S2).

To evaluate the stability of the labeling, the conjugates were incubated at 37°C in a 500-fold molar excess of EDTA for 1 h and then analyzed using radio-ITLC. The experiments were performed in duplicates. In control experiment the conjugates were incubated in PBS only.

For radioiodination of *HP2*, fifty micrograms of *HP2*, 1.1 µg/µL in PBS, was mixed with ^{125}I-iodide (15–40 MBq). The reaction was initiated by adding 5 µg Chloramine-T (1 mg/mL in PBS), and the mixture was incubated for 2 min at room temperature. The reaction was ceased by addition of 10 µl sodium metabisulfite (5 mg/mL PBS) and purified using NAP-5 columns (GE Healthcare).

To evaluate the stability of the labeling, the conjugates were incubated at 37°C in a human serum for 1 and 4 h, and then analyzed using radio-SDS-PAGE as described earlier. The experiments were performed in duplicates. In control experiment the conjugates were incubated in PBS only.

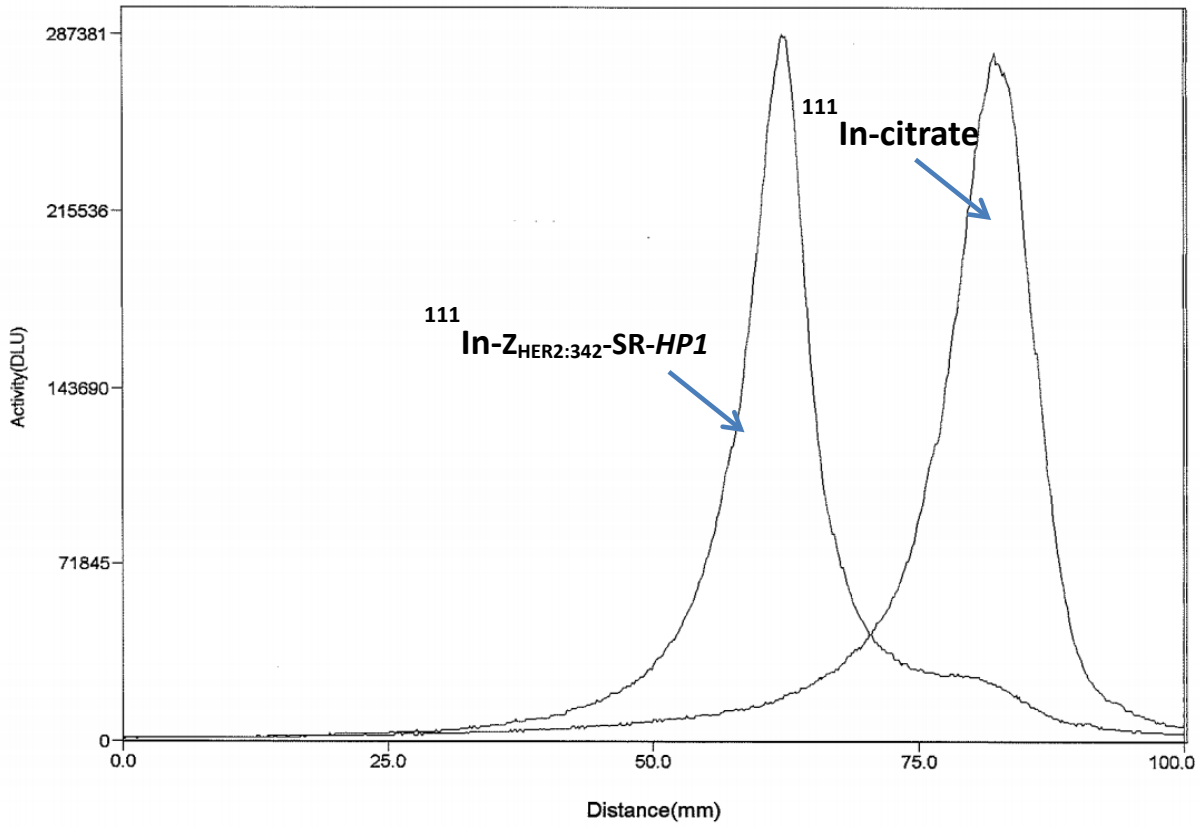

Figure S1. Distribution of radioactivity on SDS-PAGE gel showing the identity of ^{111}In-$Z_{HER2:342}$-SR-*HP1*; ^{111}In-citrate was used as a marker for low-molecular-weight compounds. The signal was measured as a digital light unit (DLU) proportional to the radioactivity in a given point of a lane in the SDS-PAGE gel.

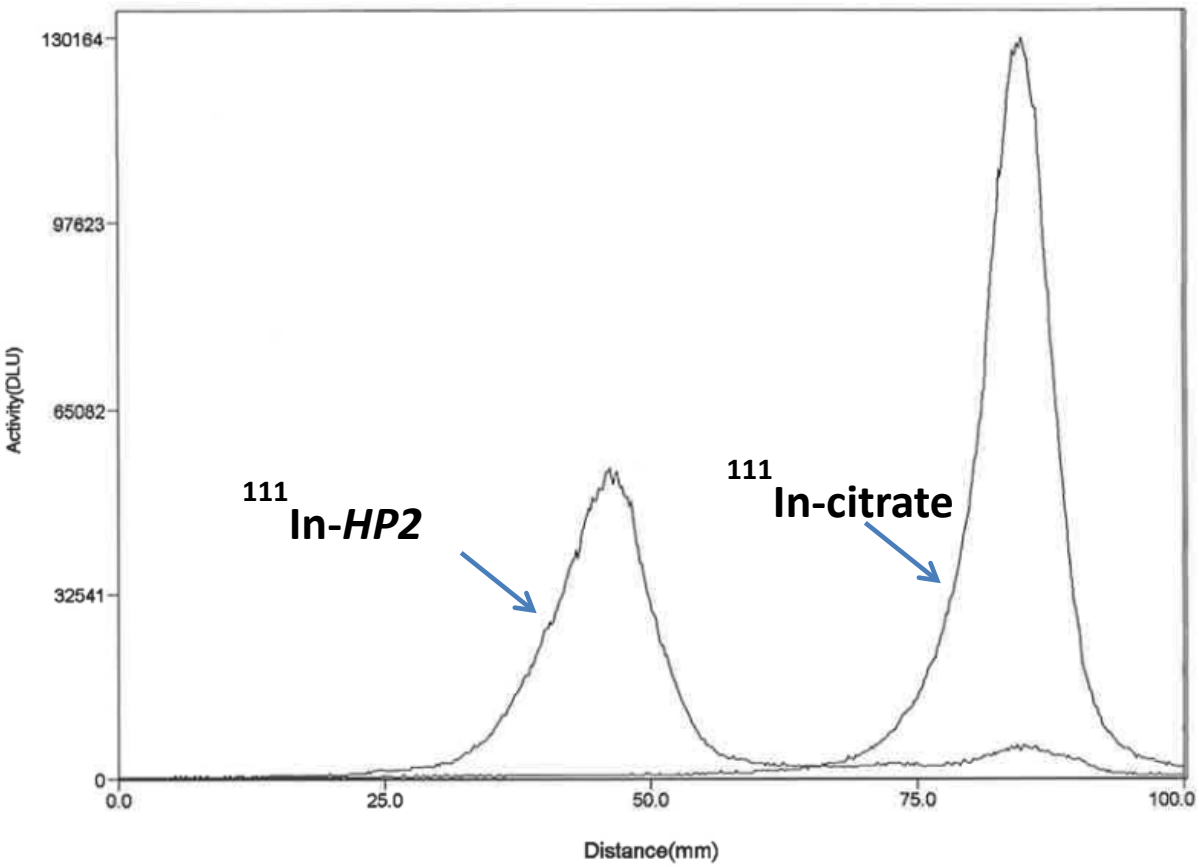

Figure S2. Distribution of radioactivity on SDS-PAGE gel showing the identity of ^{111}In-*HP2*.^{111}In-citrate was used as a marker for low-molecular-weight compounds. The signal was measured as a digital light unit (DLU) proportional to the radioactivity in a given point of a lane in the SDS-PAGE gel.

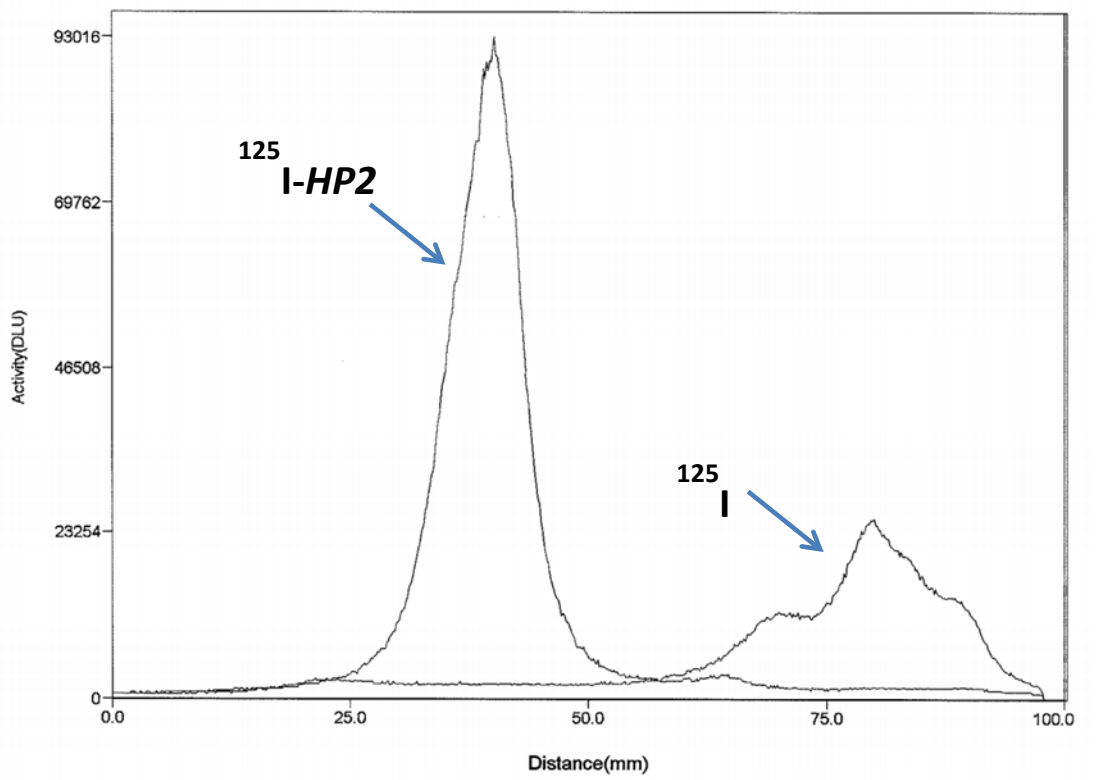

Figure S3. Representative SDS-PAGE analysis for the identity of ^{125}I-*HP2*; free ^{125}I-iodide was used as a marker for low-molecular-weight compounds. The signal was measured as a digital light unit (DLU) proportional to the radioactivity in a given point of a lane in the SDS-PAGE gel.

In vitro cell binding and processing of radiolabeled $Z_{HER2:342}$-SR-*HP1* and *HP2*

For all experiments, ca. 10^6 cells per petri dish were used. A set of three dishes was used for each data point.

The specificity of ^{111}In-$Z_{HER2:342}$-SR-*HP1* binding to HER2-expressing SKOV-3 and BT474 cells was evaluated according to the receptor saturation method described earlier (1). In addition, a HER2-negative UM-SCC74B cell line was used as a negative control. The radiolabeled conjugate (1 nM, total volume 1 mL) was added to all cell dishes. Saturation of HER2 in control samples was performed by adding 500-fold molar excess of non-labeled

parental anti-HER2 $Z_{HER2:342}$ Affibody molecule 5 min before treatment by ^{111}In-$Z_{HER2:342}$-SR-*HP1*. After 60 min incubation with ^{111}In-$Z_{HER2:342}$-SR-*HP1* at 37 °C in a humidified incubator, the incubation medium was removed and cells were washed by 2 mL fresh medium. Thereafter, cells were detached by treatment with trypsin, collected and their radioactivity was measured. For the negative control, ^{111}In-$Z_{HER2:342}$-SR-*HP1*cell binding was normalized to binding to SKOV-3 cells.

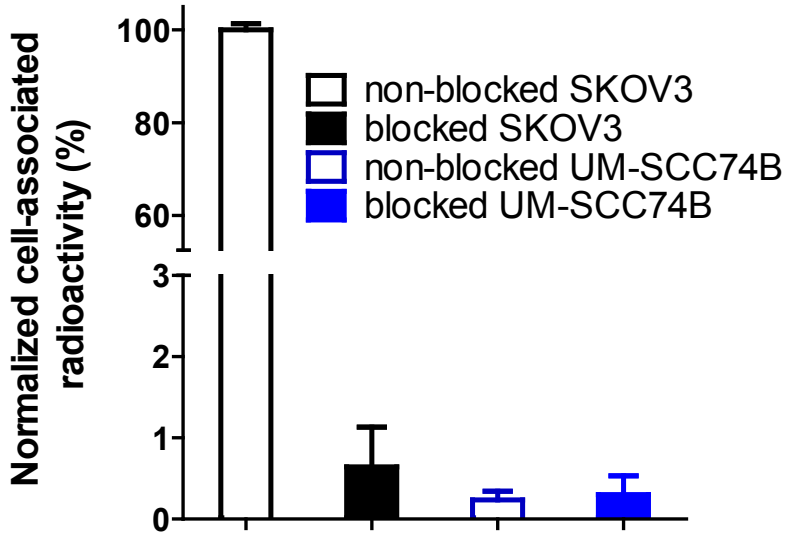

Figure S4. Comparison of ^{111}In-$Z_{HER2:342}$-SR-*HP1* binding to HER2-positive SKOV-3 cells and HER2-negative UM-SCC74B cells. Data are presented as a mean value and standard deviation for three cell culture dishes.

To demonstrate in vitro pre-targeting, HER2-expressing cells were incubated for 1 h with 1 nM $Z_{HER2:342}$-SR-HP1 (1 mL) at 37°C. Thereafter, the $Z_{HER2:342}$-SR-*HP1*-containing medium was removed and cells were washed with 2 mL fresh medium. Radiolabeled *HP2* (^{111}In-*HP2* or ^{125}I-*HP2*) was added to the cells to obtain a concentration of 10 nM in 1 mL medium, and cells were incubated at 37°C for 60 min. Cells were washed with 2 mL media, detached from petri dishes by treatment with trypsin-EDTA for 10 min, and cell-associated activity was measured. To show that binding of radiolabeled *HP2* to cells is dependent on pre-treatment with $Z_{HER2:342}$-SR-*HP1*, non-labeled parental anti-HER2 Affibody molecule (500 nM, 500-fold excess over $Z_{HER2:342}$-SR-*HP1*) was added to one set of control petri dishes 5 min before adding $Z_{HER2:342}$-SR-*HP1* to saturate receptors and prevent HER2-specific binding of $Z_{HER2:342}$-SR-*HP1*. Further treatment was as described above. To show that the PNA-PNA

interaction is essential for the binding of radiolabeled *HP2*, a non-labeled *HP2* probe (150 nM, 15-fold excess over $Z_{HER2:342}$-SR-*HP1*) was added to the cells 60 min before adding the radiolabeled *HP2* to the cells in another set of control dishes. Further treatment was as described above. To estimate unspecific binding, the radiolabeled *HP2* (10 nM) was added to cells without pre-treatment with $Z_{HER2:342}$-SR-*HP1* for 60 min. Thereafter cells were washed, detached by trypsin, and cell-associated radioactivity was measured.

To show further that binding of radiolabeled *HP2* to cells is dependent on binding of $Z_{HER2:342}$-SR-*HP1* to HER2 receptors, a HER2-negative UM-SCC74B cell line was used as a negative control. The same protocol was used for ^{125}I-*HP2* and ^{111}In-*HP2*. Six petri dishes containing ca. 10^6 UM-SCC74B cells and six dishes containing ca. 10^6 SKOV-3 cells were used for ^{125}I-*HP2* and ^{111}In-*HP2*. Non-labeled parental anti-HER2 Affibody molecule (500 nM, 500-fold excess over $Z_{HER2:342}$-SR-*HP1*) was added to one set of three control petri dishes with each cell line 5 min before adding $Z_{HER2:342}$-SR-*HP1* to saturate receptors and prevent HER2-specific binding. All cells were incubated for 1 h with 1 nM $Z_{HER2:342}$-SR-*HP1* (1 mL) at 37°C. Thereafter, the $Z_{HER2:342}$-SR-*HP1*-containing medium was removed and cells were washed with 2 mL fresh medium. Radiolabeled *HP2* (^{111}In-*HP2* or ^{125}I-*HP2*) was added to the cells to obtain a concentration of 10 nM in 1 mL medium, and cells were incubated at 37°C for 60 min. Then cells were washed, detached by trypsin, and cell-associated radioactivity was measured. Binding of ^{125}I-*HP2* and ^{111}In-*HP2* to UM-SCC74B cells was normalized to binding to SKOV-3 cells.

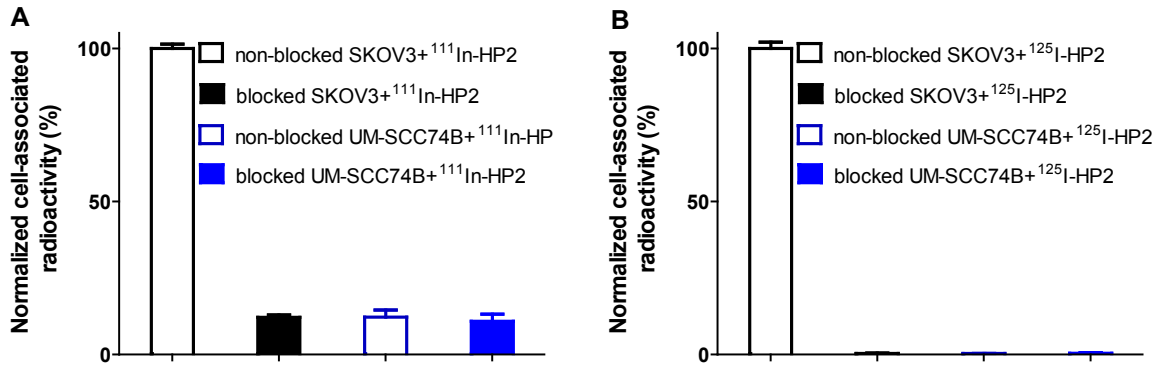

Figure S5. Comparison of ^{111}In-*HP2* (A) and ^{125}I-*HP2* (B) binding to $Z_{HER2:342}$-SR-*HP1* pre-treated HER2-positive SKOV-3 cells and HER2-negative UM-SCC74B cells. In the blocked group, receptors were saturated by adding 500-fold excess of non-labeled parental anti-HER2 Affibody molecule 5 min before adding $Z_{HER2:342}$-SR-*HP1*. Data are presented as a mean value and standard deviation for three cell culture dishes.

Cellular retention and processing of ^{111}In-$Z_{HER2:342}$-SR-*HP1* were studied using the acid-wash method validated for Affibody molecules earlier (1). Cells were incubated with 60 pM solution of ^{111}In-$Z_{HER2:342}$-SR-*HP1* at 37°C. After 1 h incubation, the medium with the labeled compound was removed and cells were washed with 2 mL serum-free medium. 1 mL of complete media was added to each dish and cells were further incubated at 37°C in a humidified incubator in an atmosphere containing 5% CO_2. At designated time points (0, 1, 2, 4, 8 and 24 h), a group of three dishes was removed from the incubator. The medium was collected and cells were washed with 2 mL ice-cold serum-free medium. Thereafter, cells were treated with 1 mL 0.2 M glycine buffer, pH 2, containing 4 M urea, for 5 min on ice. The acidic solution was collected and cells were additionally washed with 1 mL glycine buffer. The acidic fractions were pooled. The cells were then incubated with 0.5 mL 1 M NaOH at 37°C for 10 min. The cell debris was collected, and the dishes were additionally washed with 1 mL of NaOH solution. The alkaline solutions were pooled. The radioactivity in the acidic solution was considered as membrane bound, and in the alkaline fractions as internalized. 1 mL of complete media was added to each dish and cells were further incubated at 37°C in a humidified incubator in an atmosphere containing 5% CO_2. At designated time points (0, 1, 2, 4, 8 and 24 h), a group of three dishes was removed from the incubator. The medium was collected and cells were washed with 2 mL ice-cold serum-free medium. Thereafter, cells were treated with 1 mL 0.2 M glycine buffer, pH 2, containing 4 M urea, for 5 min on ice. The acidic solution was collected and cells were additionally washed with 1 mL glycine buffer. The acidic fractions were pooled. The cells were then incubated with 0.5 mL 1 M NaOH at 37°C for 10 min. The cell debris was collected, and the dishes were additionally washed with 1 mL of NaOH solution. The alkaline solutions were pooled. The radioactivity in the acidic solution was considered as membrane bound, and in the alkaline fractions as internalized.

Cellular retention and processing of $Z_{HER2:342}$-*SR-HP1*: ^{111}In-*HP2* complex by HER2-expressing cells were measured similarly. The cells were incubated with $Z_{HER2:342}$-SR-*HP1* (1 nM) at 37°C for 60 min, thereafter the media were removed and cells were washed with 2 mL fresh media. ^{111}In-*HP2* (10 nM in 1 mL) was added, and cells were incubated at 37°C for 60 min. The medium was removed and cells were washed with 2 mL fresh media.

For ^{125}I-*HP2*, only overall cellular retention was measured since radioiodine is a non-residualizing label, and the radiocatabolites are poorly retained intracellularly. The cells were incubated with $Z_{HER2:342\text{-}SR}$-*HP1* (1 nM) at 37°C for 60 min, thereafter the media were removed and cells were washed with 2 mL fresh media. ^{125}I-*HP2* (10 nM in 1 mL) was added, and cells were incubated at 37°C for 60 min. The medium was removed and cells were washed with 2 mL fresh media. At designated time points (0, 1, 2, 4, 8 and 24 h), a group of three dishes was removed from the incubator. The medium was collected and cells were washed with 2 mL ice-cold serum-free medium. Thereafter, cells were detached by treatment with trypsin, collected and their radioactivity was measured.

Affinity determination using LigandTracer

SKOV-3 human ovarian carcinoma cells were seeded on a local area of a cell culture dish (NunclonTM, Size 100620, NUNC A/S, Roskilde, Denmark), as described previously (2). The binding kinetics of the ^{111}In-$Z_{HER2:342}$-SR-*HP1* molecule to living cells was monitored in real-time at both 4°C and room temperature using LigandTracer Yellow. To measure kinetics of the interaction between $Z_{HER2:342}$-SR-*HP1* and *HP2*, the SKOV-3 cells were pre-saturated with 1 nM $Z_{HER2:342}$-SR-*HP1* for 2 h and thereafter washed three times to remove unbound $Z_{HER2:342}$-SR-*HP1*. The binding of ^{111}In-*HP2* was measured using LigandTracer Yellow, and the binding of ^{125}I-*HP2* by LigandTracer Grey, with both measurements performed at room temperature.

The LigandTracer devices record the kinetics of binding and dissociation of radiolabeled tracers to and from receptors on living cells. The InteractionMap software (2) was used to calculate both the association and dissociation rates and to determine the affinities of radiolabeled conjugates. In order to cover the concentration span needed for proper affinity estimation, two increasing concentrations of each radioconjugate, ^{111}In-$Z_{HER2:342}$-SR-*HP1* (60, and 180 pM), ^{111}In-*HP2* (5 and 15 nM), and ^{125}I-*HP2* (2 and 6 nM) were added in each affinity assay. Analysis was performed in duplicates.

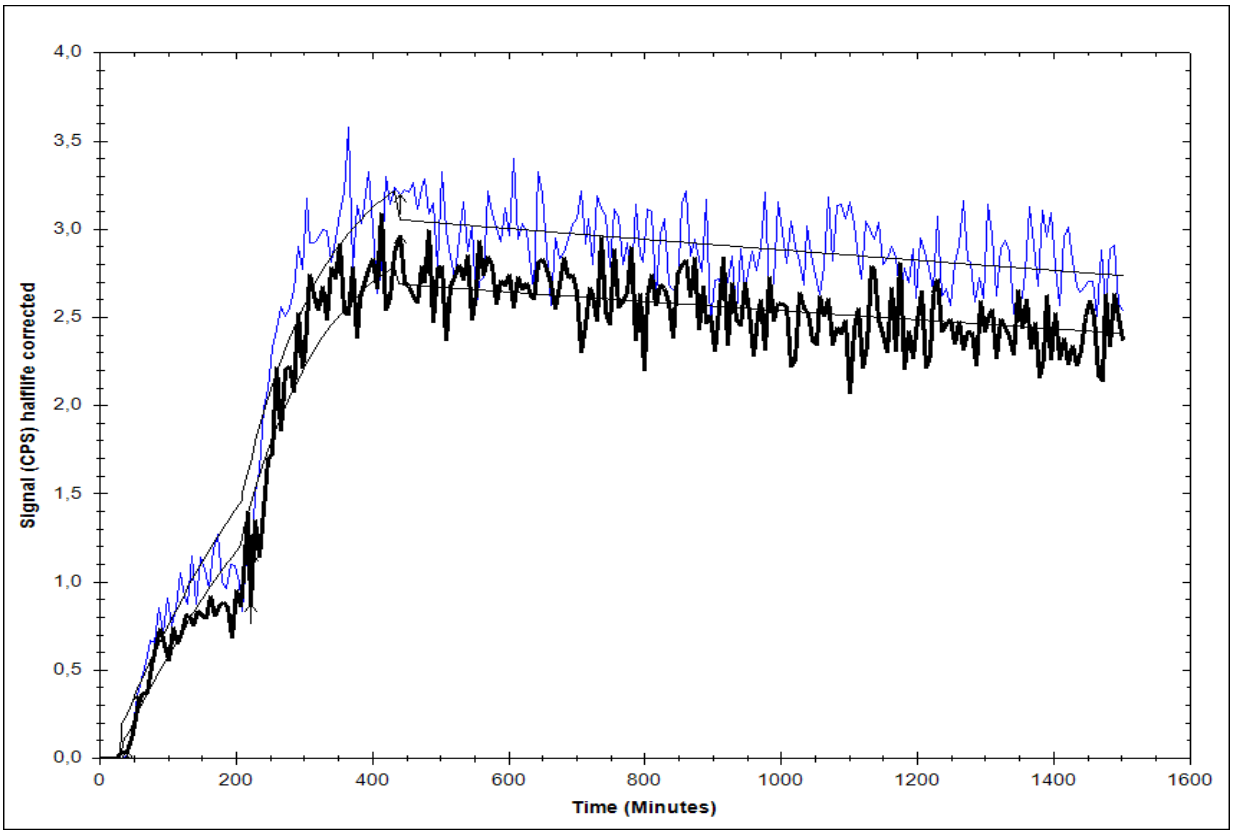

Figure S6. Binding curves (LigandTracer Yellow sensorgrams) representing the interaction of ^{111}In- $Z_{HER2:342}$-SR-*HP1* with HER2-expressing SKOV-3 cells at room temperature. Duplicate measurements (blue and black sensorgrams) were superimposed for kinetic evaluations.

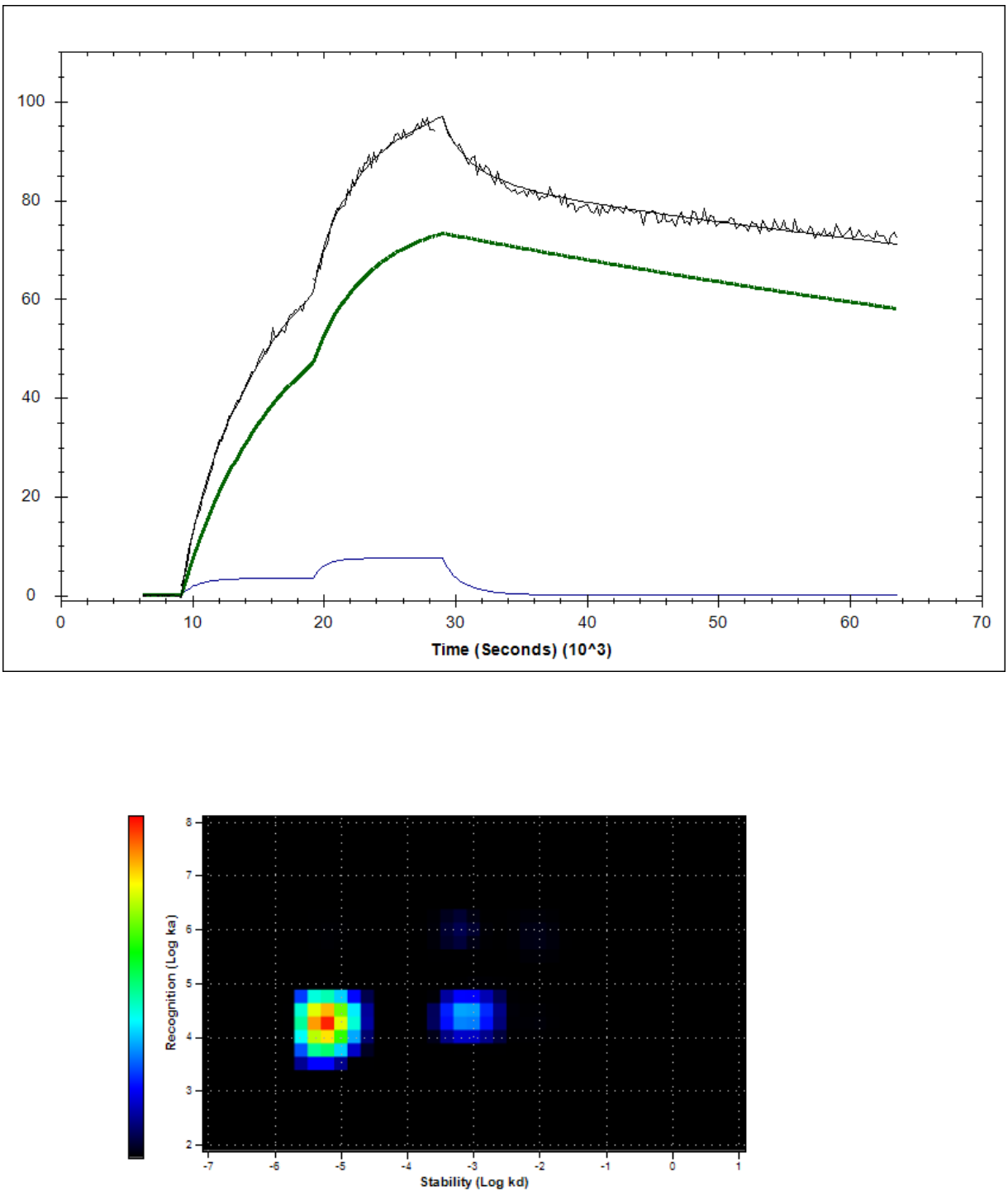

Figure S7. Upper panel. Binding curves (LigandTracer Yellow sensorgrams) representing the interaction of ^{111}In-*HP2* with HER2-expressing SKOV-3 cells pre-treated with $Z_{HER2:342}$-SR-*HP1* at two different concentrations. Fitting binding curves to 1:2 interaction models indicates two interactions, one low nanomolar and one picomolar. **Lower panel:** Interaction Maps illustrating the heterogeneity of the interactions. Two different interactions are visible, one with lower and one with higher off-rate.

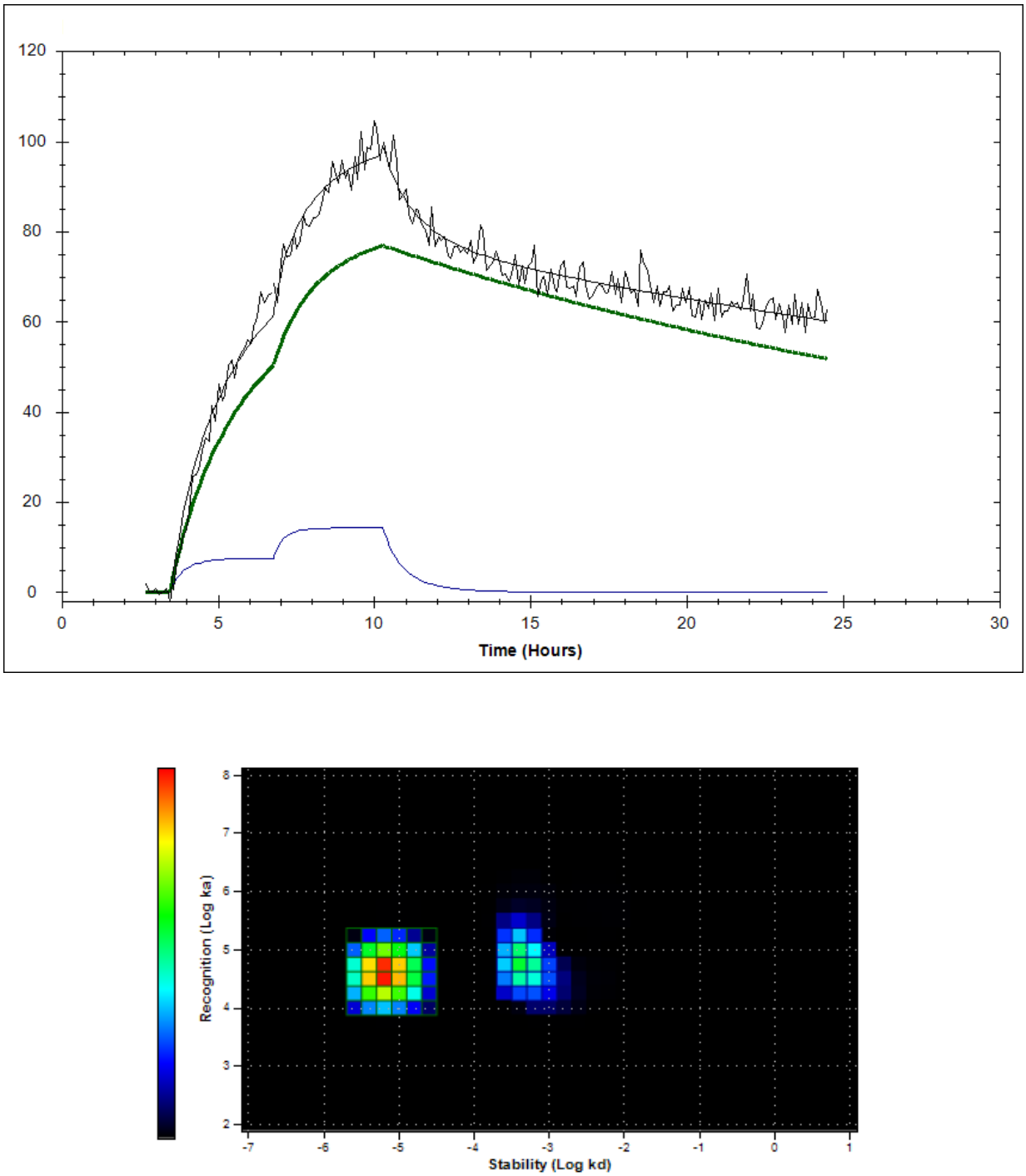

Figure S8. Upper panel: Binding curves (LigandTracer Gray sensorgrams) representing the interaction of ^{125}I-*HP2* with HER2-expressing SKOV-3 cells pre-treated with $Z_{HER2:342}$-SR-*HP1* at two different concentrations. Fitting binding curves to 1:2 interaction models indicates two interactions, one low nanomolar and one picomolar. **Lower panel**: Interaction Maps illustrating the heterogeneity of the interactions. Two different interactions are visible, one with lower and one with higher off-rate.

Biodistribution in normal mice after subcutaneous and intravenous injection

Table S1. In vivo comparison of biodistribution of ^{111}In-$Z_{HER2:342}$-SR-*HP1* in NMRI mice after intravenous (IV) and subcutaneous (SC) injection. Data are presented as an average % ID/g and standard deviation for 4 mice. Data for gastrointestinal tract (with content) and carcass are presented as %ID per whole sample.

	1h SC	**4h SC**	**8h SC**	**1h IV**	**4h IV**	**8h IV**
Blood	1.93±0.08	0.32±0.11	0.15±0.02	0.79±0.08*	0.16±0.02*	0.14±0.05
Lung	1.16±0.04	0.30±0.05	0.18±0.02	0.80±0.04*	0.32±0.06	0.27±0.08
Liver	0.57±0.03	0.63±0.10	0.59±0.03	1.1±0.1*	1.0±0.1*	0.9±0.3
Spleen	0.41±0.06	0.22±0.03	0.24±0.04	0.43±0.04	0.34±0.04*	0.4±0.1
Pancreas	0.41±0.05	0.15±0.03	0.33±0.36	0.28±0.07*	0.14±0.01	0.20±0.09
Stomach	0.75±0.12	0.33±0.08	0.20±0.01	0.46±0.07*	0.3±0.2	0.23±0.08
Colon	0.72±0.08	0.26±0.06	0.21±0.01	0.48±0.04*	0.26±0.04	0.25±0.09
Kidney	149±32	129±14	255±17	240±19*	231±51*	245±18
Muscle	0.36±0.03	0.18±0.09	0.08±0.00	0.28±0.04*	0.12±0.01	0.12±0.05
Bones	0.60±0.09	0.33±0.06	0.25±0.06	0.56±0.04	0.39±0.08	0.37±0.08
Brain	0.05±0.01	0.01±0.01	0.00±0.00	0.03±0.01	0.01±0.00	0.01±0.00
GI	1.2±0.2	0.9±0.4	0.6±0.2	0.72±0.08*	0.7±0.3	0.8±0.5
Carcass	45±7	17±3	12±2	7.1±0.9*	3.3±0.5	3.1±0.8

*Difference was significant ($p < 0.05$) between biodistribution after sc and iv injection at the same time point.

Table S2. Biodistribution of ^{125}I-*HP2* and ^{111}In-*HP2* (1 μg) in BALB/C nu/nu mice bearing SKOV-3 xenografts at 1 h p.i. $Z_{HER2:342}$-SR-*HP1* (100 μg) was pre-injected 4 h prior to the injection of *HP2*. Data are presented as an average value with standard deviation for 5 mice.

%ID/g	^{111}In-*HP2* (1 μg)	^{125}I-*HP2* (1 μg)
Blood	0.42±0.27*	2.1±0.5
Lung	0.85±0.23*	3.2±0.9
Liver	0.30±0.04*	1.0±0.3
Spleen	0.27±0.06*	1.0±0.2
Kidney	10.76±2.13*	5.6±1.2
Tumor	18.50±1.50	19±8
Muscle	0.17±0.07*	0.6±0.3
Bones	0.20±0.10	0.5±0.3

* Difference was significant ($p < 0.05$) in ^{111}In- *HP2* and ^{125}I-*HP2* in SKOV-3 xenografts at 1 h p.i.

Table S3. Tumor-to-organ ratio of ^{125}I-*HP2* and ^{111}In-*HP2* (1 μg) in BALB/C nu/nu mice bearing SKOV-3 xenografts at 1 h p.i. $Z_{HER2:342}$-SR-*HP1* (100 μg) was pre-injected 4 h prior to injection of *HP2*. Data are presented as an average value with standard deviation for 5 mice.

	^{111}In-*HP2*	^{125}I-*HP2*
Blood	54±19	9±3*
Lung	23±6	6±2*
Liver	62±9	19±5*
Spleen	72±17.08	19±6*
Kidney	1.8±0.3	3.3±0.9*
Muscle	123±38	30±17*
Bones	118±63	53±36*

* Difference was significant ($p < 0.05$) in tumor-to-organ ratio of ^{111}In-*HP2* and ^{125}I-*HP2* in SKOV-3 xenografts at 1 h p.i.

Supporting References

1. Wållberg H, Orlova A. Slow internalization of anti-HER2 synthetic affibody monomer ^{111}In-DOTA-$Z_{HER2:342}$-pep2: implications for development of labeled tracers. Cancer Biother Radiopharm. 2008; 23: 435–442.

2. Björkelund H, Gedda L, Barta P, Malmqvist M, Andersson K. Gefitinib induces epidermal growth factor receptor dimers which alters the interaction characteristics with ^{125}I-EGF. PLoS One 2005; 6.